A conserved water-mediated hydrogen bond network defines bosutinib's kinase selectivity

Nicholas M. Levinson[1*] **and Steven G. Boxer**[1]

[1]Department of Chemistry, Stanford University, Stanford, California, United States of America

*To whom correspondence should be addressed. Email: nickl@stanford.edu

Supplementary Information

Supplementary Results

Supplementary Table 1. X-ray data collection and refinement statistics.

	Src WT	Src A403T	Src T338M/M314L
Data collection			
Space group	P1	P1	P1
Cell dimensions			
a, *b*, *c* (Å)	41.9, 63.2, 73.7	41.8, 63.1, 78.3	41.9, 63.1, 74.3
α, β, γ (°)	79.5, 89.3, 90.1	79.5, 89.2, 90	78.5, 87.5, 89.8
Resolution (Å)	72-2.1*	62-2.6	72-2.6*
R_{sym} or R_{merge}	0.145 (0.539)	0.121 (0.487)	0.195 (0.475)
I / σI	5.8 (2.1)	5.6 (1.7)	4.4 (2.1)
Completeness (%)	95.9 (93.8)	91.8 (92.5)	95.8 (94.2)
Redundancy	3.2	1.9	3.1
Refinement			
Resolution (Å)	2.1	2.6	2.6
No. reflections	41303	20889	21929
R_{work} / R_{free}	0.21/0.25	0.21/0.28	0.21/0.27
No. atoms			
Protein	4278	4238	4272
Ligand/ion	64	64	64
Water	284	91	66
B-factors			
Protein	34.7	37.75	41.8
Ligand/ion	35.1	41.2	54.6
Water	32.6	27.9	29.5
R.m.s. deviations			
Bond lengths (Å)	0.008	0.009	0.009
Bond angles (°)	1.084	1.225	1.173
PDB accession code	4MXO	4MXX	4MXZ

Values in parentheses are for highest-resolution shell.
*data merged from 2 crystals.

Supplementary Table 2. IR and binding data for all Src mutants.

Src mutant	CN Frequency	Kd(nM)
T338M/A403S	2213.1	20.8
T338M/A403T/V323T	2213.1	43
T338M/A403T	2213.4	20.2
T338L	2213.7	67
T338M/M314L	2213.8	21.2
T338M/V323T	2213.9	21
T338M	2214.6	20
V323C/A403T	2215.7	48
T338N	2215.8	70
T338M/A403C	2215.8	23
T338I	2215.9	225
T338F	2216.0	18.5
V323S/A403T	2216.9	37
T338Q	2217.0	279
A403T	2217.3	29
T338I/M314L	2217.4	578
T338V	2217.9	11
V323S	2218.4	2.3
V323C	2219.2	1.5
V323T	2219.8	0.8
A403V	2220.0	0.4
V323L	2220.7	22.9
A403C	2221.5	0.4
M314L	2221.5	2.8
T338S	2222.2	6.1
M314H	2222.8	5.7
A403S	2223.2	0.42
WT	2223.6	0.73
M314T	2224.1	3.02
M314C	2224.6	9.32
M314Q	2224.6	7.78
M314S	2225.6	2.04
M314Y	2225.6	7.95

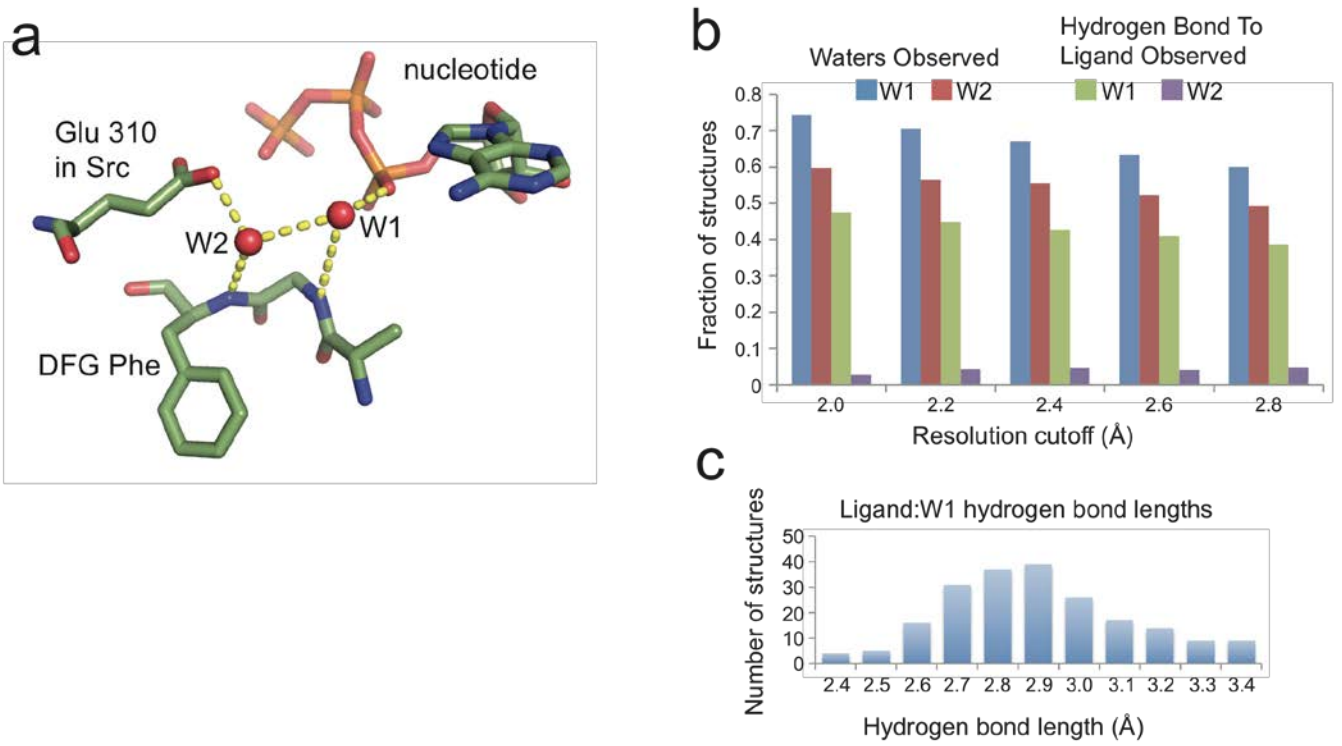

Supplementary Figure 1. Data from our analysis of structures in the protein databank. (**a**) Structure of the cyclin-dependent kinase 2 bound to nucleotide and activating cyclin (pdb code 1JST). Hydrogen bonds are shown as dashed yellow lines. (**b**) Statistical data from our analysis of 630 kinase/inhibitor complexes. The graph shows the frequencies with which waters W1 and W2 are observed, as well as the frequencies with which they are engaged in hydrogen bonds by the ligand, as a function of different resolution cutoffs. (**c**) The distribution of hydrogen bond lengths for 180 ligand/W1 hydrogen bonds.

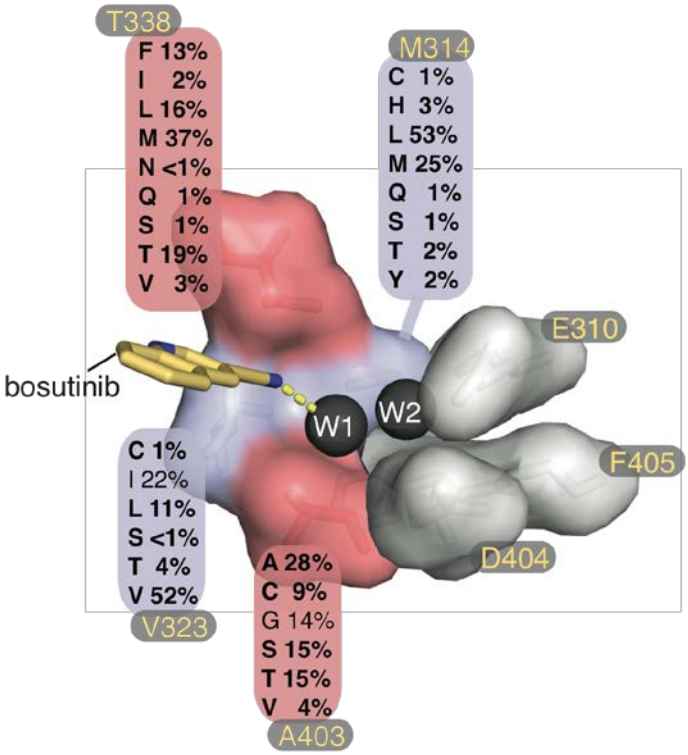

Supplementary Figure 2. Cavity-lining residues mutated in this work. A surface representation of the water-filled cavity is shown. For each cavity-lining position, the frequency with which each amino acid is found in human kinases is shown using the single letter amino acid code. Some rare substitutions are not shown. Substitutions for which IR and binding data were obtained are shown in bold. The Src numbering is shown in yellow for each position. W1 and W2 are shown as black spheres. The quinoline-3-carbonitrile moiety of bosutinib is shown as gray sticks, and the hydrogen bond between the nitrile and W1 as a dotted yellow line. The data are derived from a sequence alignment of the human kinome[1].

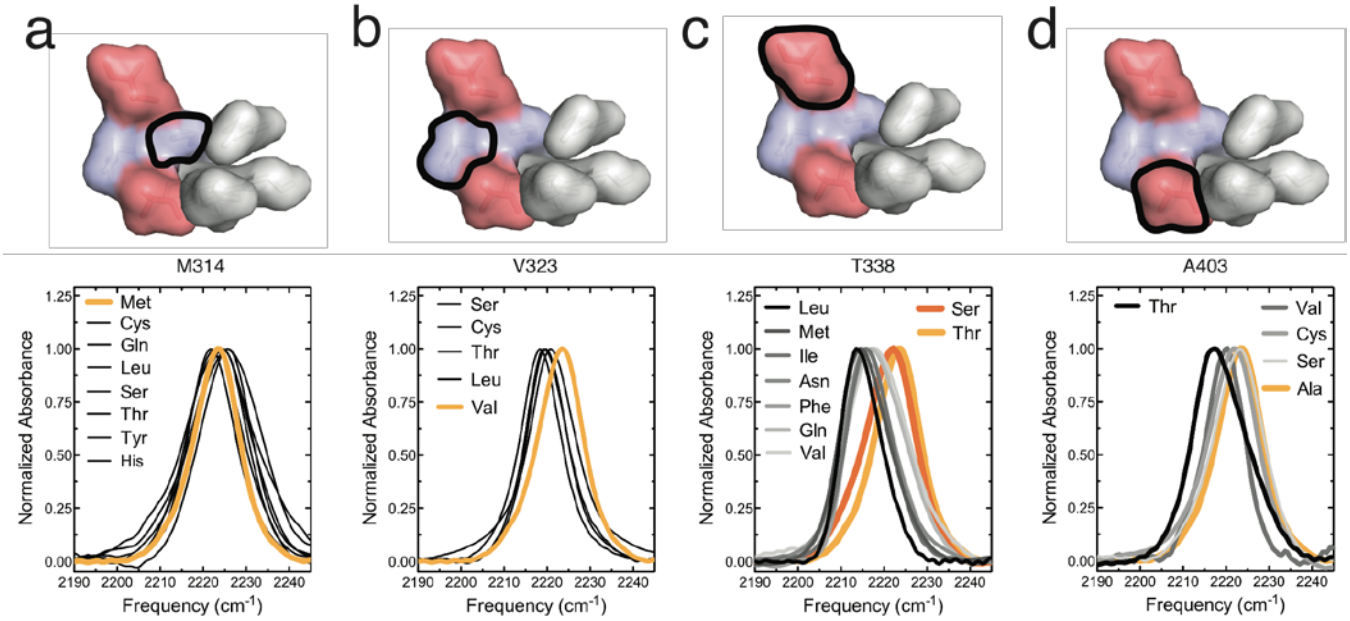

Supplementary Figure 3. IR spectra of all Src mutants. (**a**) Position 314. (**b**) Position 323. (**c**) Position 338. (**d**) Position 403. Above each panel of spectra a surface representation of the water-filled cavity is shown with the position mutated highlighted with a thick black line.

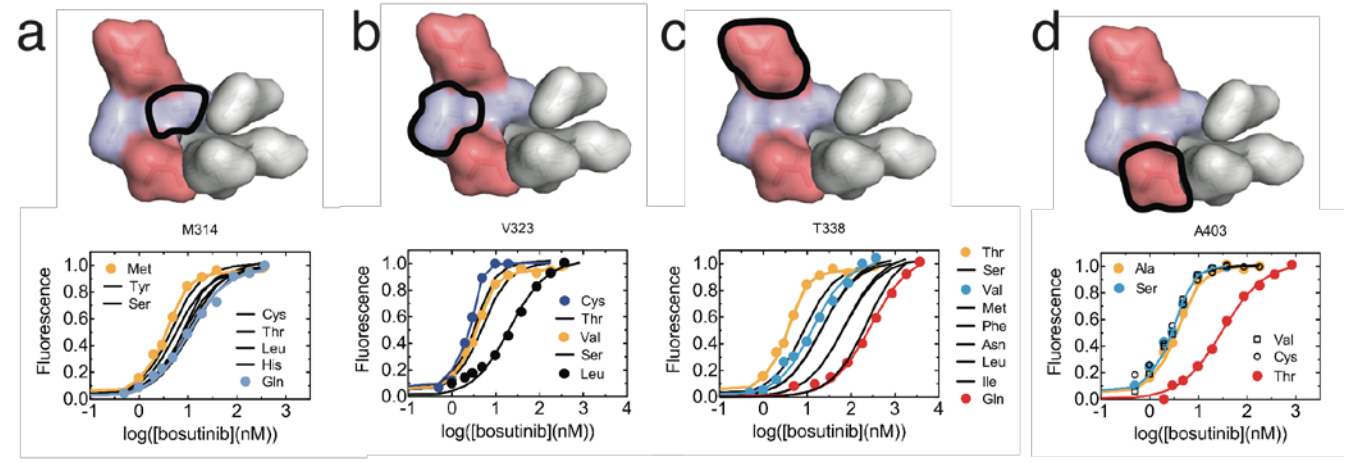

Supplementary Figure 4. Fluorescence binding measurements for all Src mutants. (**a**) Position 314. (**b**) Position 323. (**c**) Position 338. (**d**) Position 403. The fluorescence decrease at 340 nm with excitation at 280 nm is plotted as a function of the bosutinib concentration. Above each panel of binding curves a surface representation of the water-filled cavity is shown with the position mutated highlighted with a thick black line. Binding curves have been normalized to a maximum fluorescence of 1.

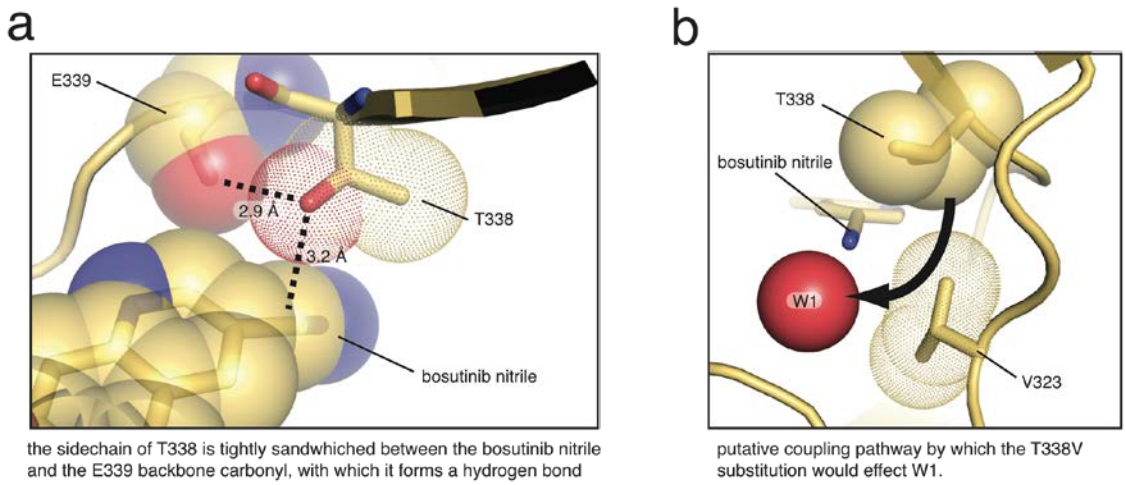

Supplementary Figure 5. Putative mechanism for disruption of the hydrogen bond network by the T338V substitution. (**a**) View of the interactions between the sidechain of T338, the backbone carbonyl of E339, and the nitrile group of bosutinib in the crystal structure of WT Src bound to bosutinib. (**b**) View of the same structure rotated by 90 degrees about the vertical axis. The thick black arrow denotes a possible pathway by which the effects of the T338V substitution might be coupled to W1, via the sidechain of V323.

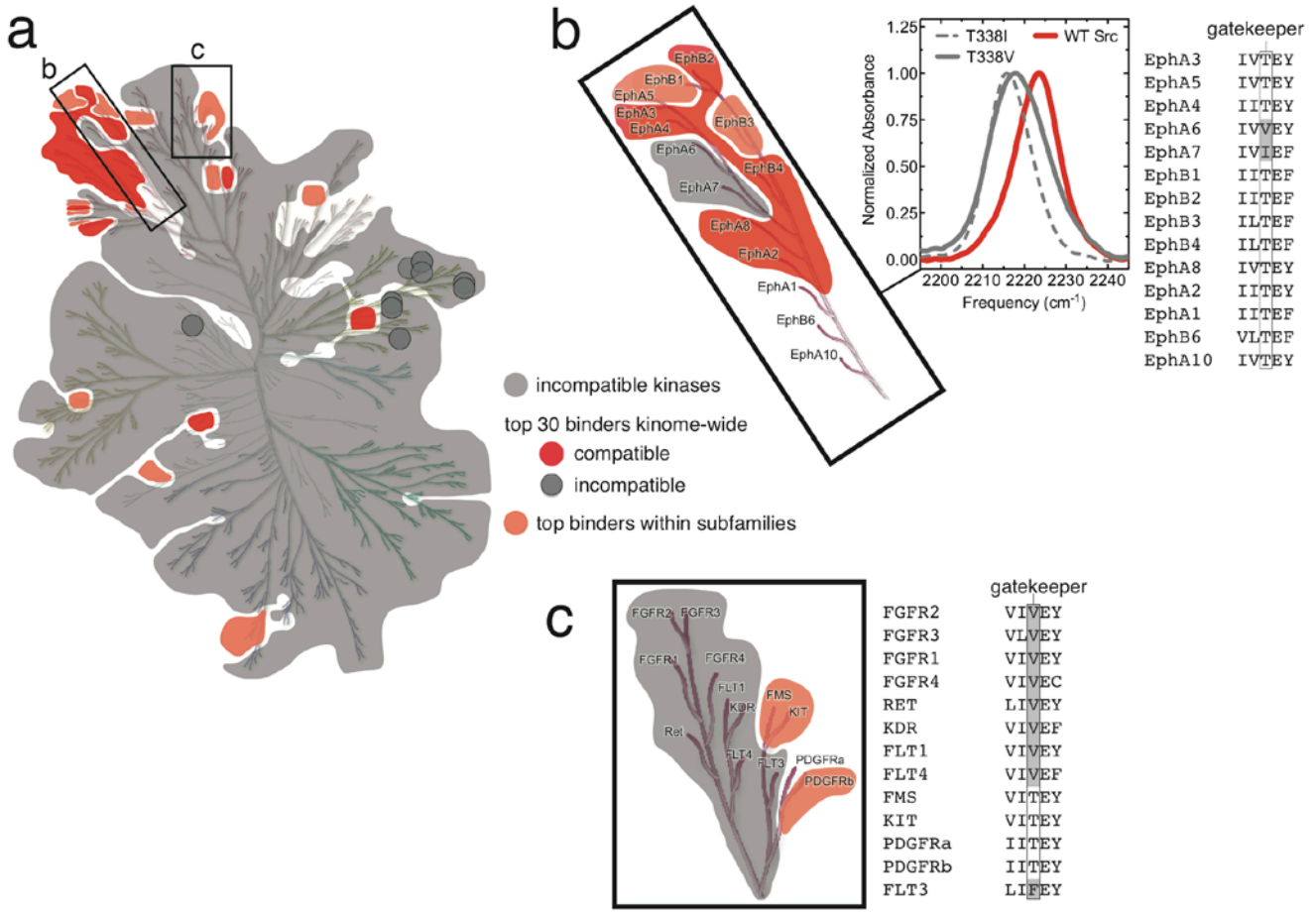

Supplementary Figure 6. The impact of the hydrogen bond network on bosutinib binding is reflected in the selectivity profile of bosutinib. (**a**) Phylogenetic tree of the human kinome taken from the main manuscript, in which kinases with ATP-binding sites that are not compatible with bosutinib's participation in the hydrogen bond network are shaded gray, kinases that bind tightly to bosutinib are colored bright red or dark gray, and kinases for which bosutinib displays subfamily selectivity are colored light red. The binding data is taken from Davis et al.[2] (reference 16 in the main text). (**b**) Enlarged view of the phylogenetic tree showing the Ephrin receptor family, along with a sequence alignment showing the residues found at the gatekeeper position in this kinase subfamily, and IR spectra of bosutinib bound to WT Src and the T338I and T338V gatekeeper mutants of Src. The coloring is the same as in a. (**c**) Enlarged view of the phylogenetic tree showing the PDGFR, VEGFR and FGFR subfamilies, along with a sequence alignment showing the residues found at the gatekeeper position in these subfamilies. The coloring is the same as in a. The phylogenetic tree of the human kinome is reproduced with permission from Cell Signaling Technologies.

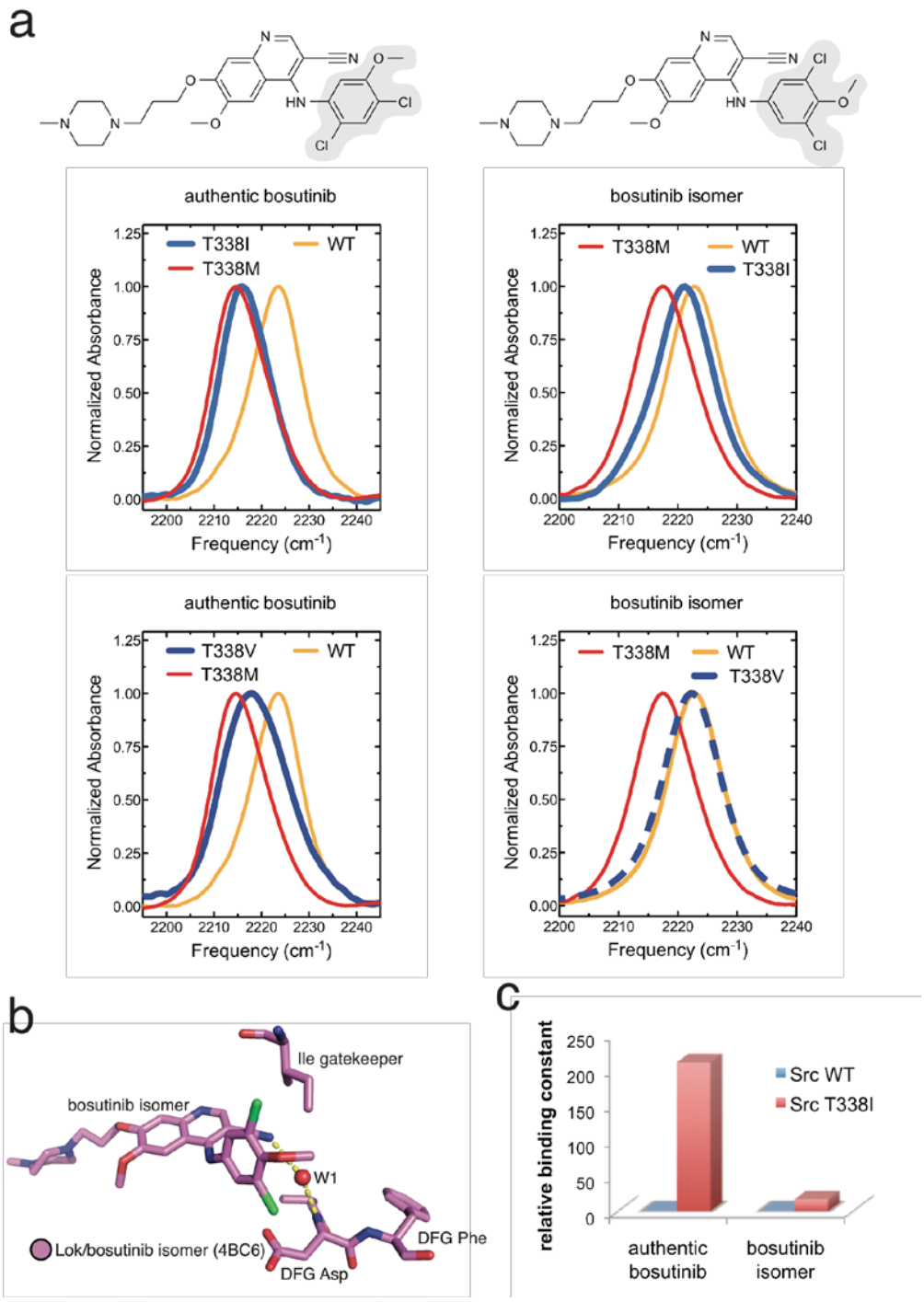

Supplementary Figure 7. Authentic bosutinib and the bosutinib isomer respond differently to substitutions of the gatekeeper. (**a**) IR spectra of authentic bosutinib and the bosutinib isomer bound to WT Src (yellow), the T338M gatekeeper substitution (red), and the T338I (top) and T338V (bottom) gatekeeper substitutions (blue). The chemical structures of authentic bosutinib and the bosutinib isomer are shown above the IR spectra. (**b**) The crystal structure of the ser/thr kinase LOK bound to the bosutinib isomer (pdb code 4BC6). The isoleucine gatekeeper is highlighted, and the hydrogen bond between the nitrile and W1 is shown as a yellow dashed line. (**c**) Binding data for authentic bosutinib and the bosutinib isomer measured with WT Src and Src T338I. The y-axis shows the fold change in the dissociation constant upon making the T338I substitution. This highlights that the Ile gatekeeper substitution has a much more severe effect on binding for authentic bosutinib than for the isomer, presumably because the hydrogen bond network is retained in the latter.

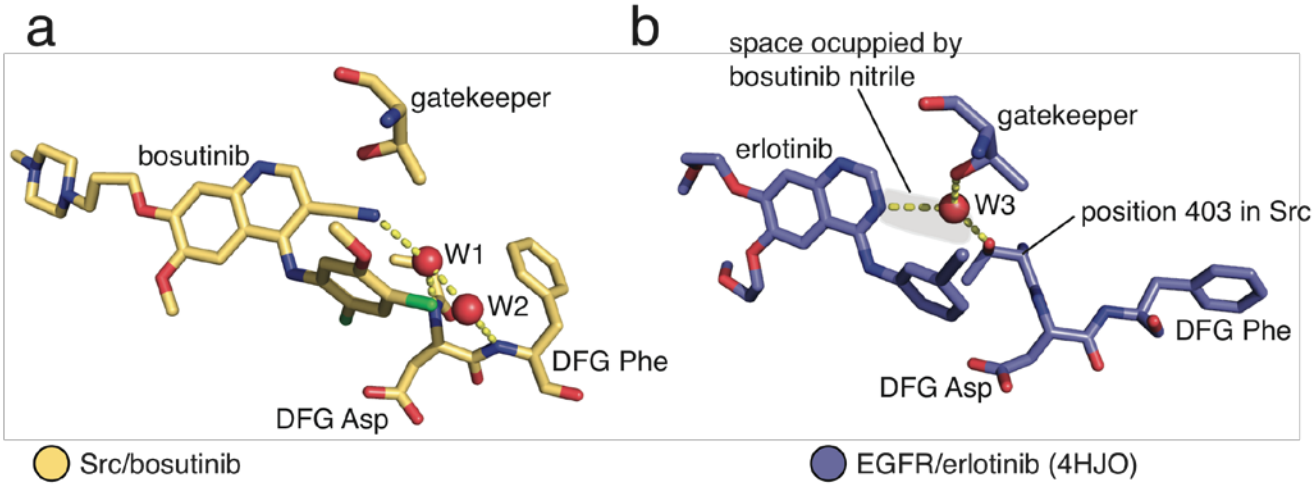

Supplementary Figure 8. Comparison between the binding modes of bosutinib and the chemically related 4-anilinoquinazoline inhibitors. (**a**) Our structure of bosutinib bound to WT Src, showing the manner in which the nitrile engages W1 in a hydrogen bond. (**b**) The structure of the 4-anilinoquinazoline inhibitor erlotinib bound to EGFR (pdb code 4HJO), in the same orientation as A. The space that would be occupied by the nitrile of bosutinib is shown as a transparent gray oval. Water molecule W3 takes the place of the bosutinib nitrile in the EGFR/erlotinib structure, and forms a hydrogen bond both to the threonine gatekeeper and to the threonine residue found at the position equivalent to A403 in Src. Hydrogen bonds are shown as dashed yellow lines.

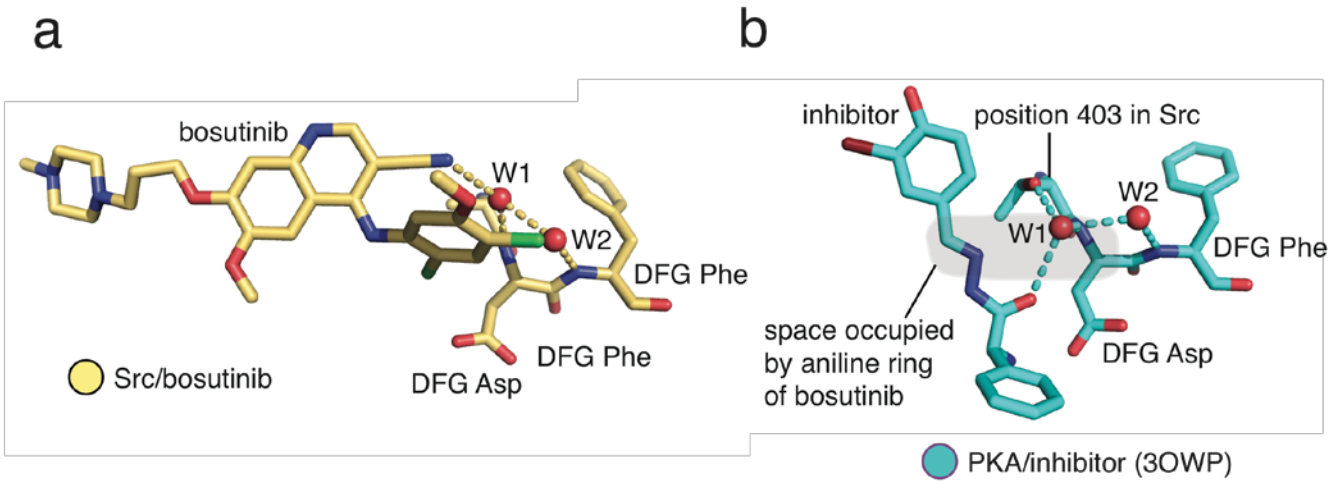

Supplementary Figure 9. Implications of the A403T substitution for inhibitors that access the water-mediated hydrogen bond network. (**a**) Our structure of bosutinib bound to WT Src, showing the manner in which the nitrile engages W1 in a hydrogen bond. (**b**) A structure of a type I inhibitor bound to PKA (pdb code 3OWP), identified in our search of the protein databank, in which a carbonyl on the inhibitor forms a hydrogen bond to W1 in the presence of a threonine residue at the position equivalent to A403 in Src. The space that would be occupied by the aniline ring of bosutinib is shown as a transparent gray oval.

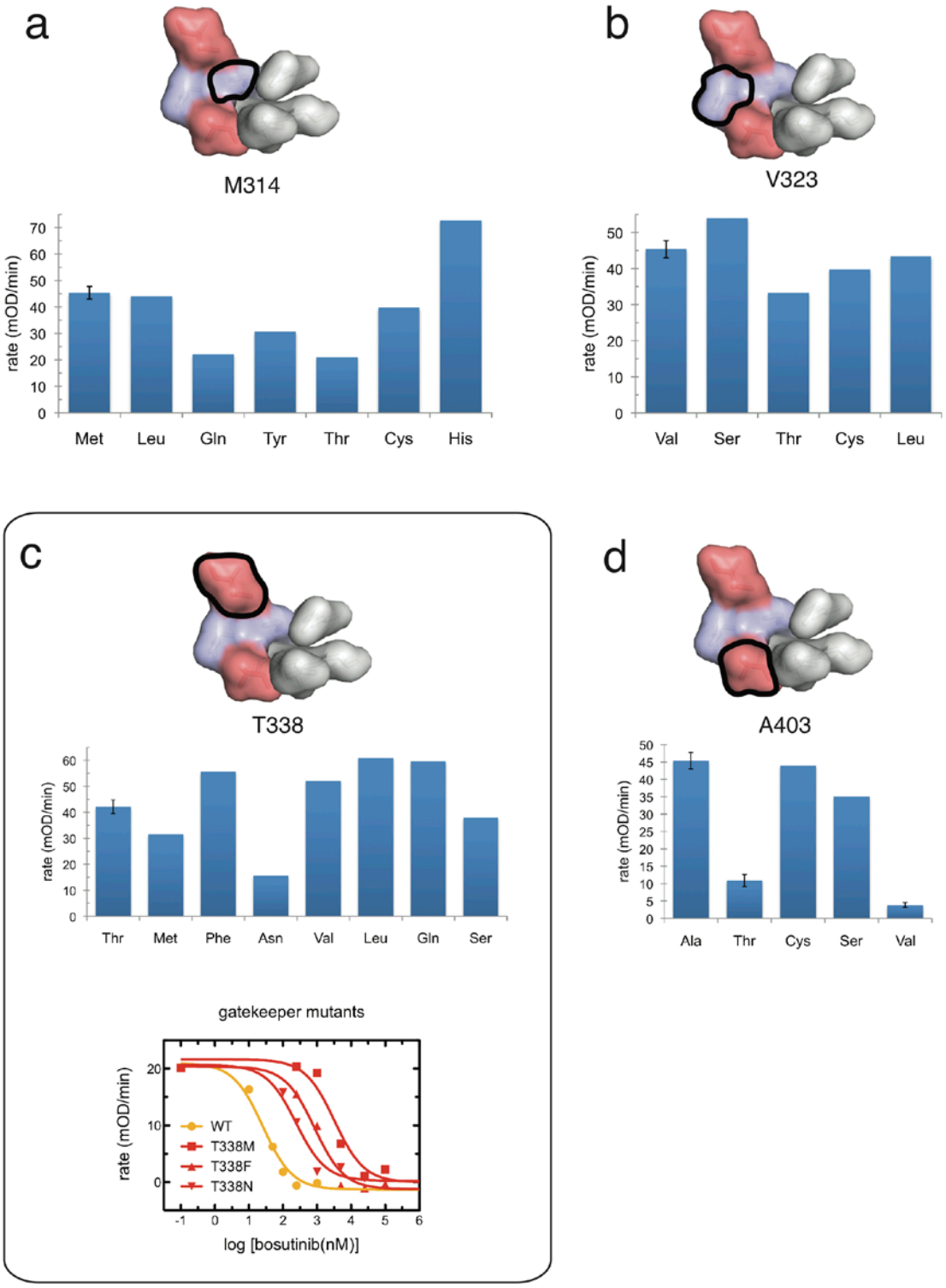

Supplementary Figure 10. Kinase activity assays of selected Src mutants. (**a**) Position 314. (**b**) Position 323 (**c**) Position 338. (**d**) Position 403. The bar graphs show kinase activity measurements performed at 200 nM kinase and 500 μM ATP. In c the effect of bosutinib on kinase activity is shown for selected mutants, measured using 100 nM kinase and 500 μM ATP, where the activities of the mutants in the absence of bosutinib were normalized to that of WT to facilitate comparison. Above each panel of bar graphs a surface representation of the water-filled cavity is shown with the position mutated highlighted with a thick black line.

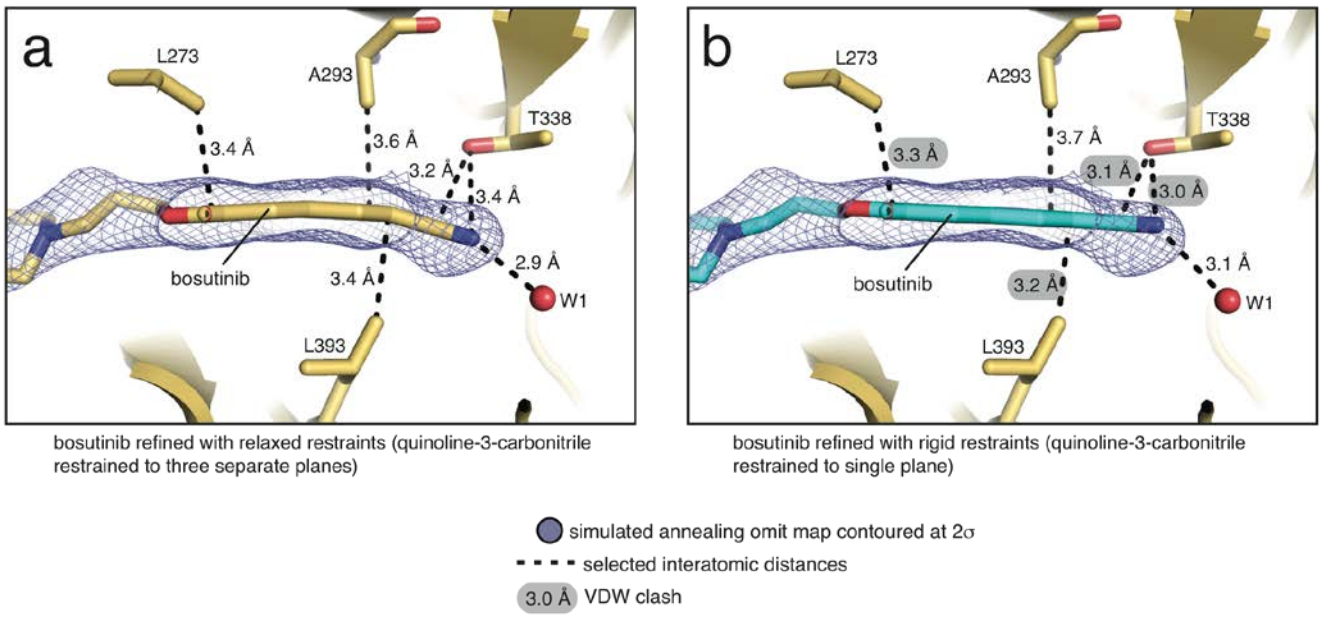

Supplementary Figure 11. **Buckling of the quinoline-3-carbonitrile moiety of bosutinib in the structure of the drug bound to Src.** (**a**) The structure refined with relaxed restraints as indicated below the panel. (**b**) The structure refined with rigid restraints as indicated below the panel. The blue mesh is a simulated annealing omit map, which represents the electron density corresponding to bosutinib without phase bias from the model of the drug itself. Relevant interatomic distances are indicated, and significant van der Waals clashes are highlighted in bold type on a gray background and indicate that the buckling of the drug relieves clashes with four ATP-binding site residues.

References

1. Manning, G., Whyte, D.B., Martinez, R., Hunter, T. & Sudarsanam, S. The protein kinase complement of the human genome. *Science* **298**, 1912-1934 (2002).
2. Davis, M.I., *et al.* Comprehensive analysis of kinase inhibitor selectivity. *Nat Biotechnol* **29**, 1046-1051 (2011).